Computer Physics Communications 270 (2022) 108153

Contents lists available at ScienceDirect

Computer Physics Communications

www.elsevier.com/locate/cpc

MagneticTB: A package for tight-binding model of magnetic and non-magnetic materials [☆],[☆☆]

Zeying Zhang [a], Zhi-Ming Yu [b,c], Gui-Bin Liu [b,c,*], Yugui Yao [b,c,*]

[a] College of Mathematics and Physics, Beijing University of Chemical Technology, Beijing 100029, China
[b] Centre for Quantum Physics, Key Laboratory of Advanced Optoelectronic Quantum Architecture and Measurement (MOE), School of Physics, Beijing Institute of Technology, Beijing, 100081, China
[c] Beijing Key Lab of Nanophotonics & Ultrafine Optoelectronic Systems, School of Physics, Beijing Institute of Technology, Beijing, 100081, China

ARTICLE INFO

Article history:
Received 20 May 2021
Received in revised form 23 August 2021
Accepted 29 August 2021
Available online 6 September 2021

Keywords:
Tight-binding method
Representation theory
Magnetic space group
Mathematica

ABSTRACT

We present a Mathematica program package MagneticTB, which can generate the tight-binding model for arbitrary magnetic space group. The only input parameters in MagneticTB are the (magnetic) space group number and the orbital information in each Wyckoff position. Some useful functions including getting the matrix expression for symmetry operators, manipulating the energy band structure by parameters, and interfacing with other software are also developed. MagneticTB can help to investigate the physical properties in both magnetic and non-magnetic system, especially for topological properties.

Program summary
Program Title: MagneticTB
CPC Library link to program files: https://doi.org/10.17632/kws9xbvz3y.1
Developer's repository link: https://github.com/zhangzeyingvv/MagneticTB
Licensing provisions: GNU General Public Licence 3.0
Programming language: Mathematica
External routines/libraries: ISOTROPY (iso.byu.edu)
Nature of problem: Construct the symmetry adapted tight-binding model for the system with arbitrary magnetic space group.
Solution method: The symmetry-adapted tight-binding model in this code is based on the Bloch theorem and group representation theory.
Additional comments including restrictions and unusual features: This code supports the spinless system and spinful system with collinear or non-collinear magnetization configuration.

1. Introduction

Tight-binding method is a powerful tool to investigate the novel properties in condensed matter physics [1–5]. Compared with first-principles method, tight-binding method can greatly simplify calculations. Moreover, after considering (magnetic) space group symmetry, the tight-binding model can give more reliable results. For example, in topological materials, symmetry plays an important role to protect the topological properties, such as Z_2 topological insulator protected by time-reversal symmetry [6], topological crystalline insulators and topological nodal semimetals protected by space group symmetries [7,8] and magnetic topological crystalline insulator protected by magnetic space group symmetries, i.e. the combination of space group operations and time-reversal [9,10].

In general, the tight-binding method can be used for both magnetic and non-magnetic systems, some packages have already been developed to solve the magnetic problem. For examples, TB-LMTO program [11,12] based on the tight-binding linear muffin-tin orbital method,

[☆] The review of this paper was arranged by Prof. Blum Volker.
[☆☆] This paper and its associated computer program are available via the Computer Physics Communications homepage on ScienceDirect (http://www.sciencedirect.com/science/journal/00104655).
[*] Corresponding authors.
E-mail addresses: gbliu@bit.edu.cn (G.-B. Liu), ygyao@bit.edu.cn (Y. Yao).

https://doi.org/10.1016/j.cpc.2021.108153
0010-4655/© 2021 Elsevier B.V. All rights reserved.

DFTB+ package has implemented density functional based tight-binding model and can do the large-scale simulations [13], SPR-TB-KKR use the Green function formalism and atomic sphere approximation which has advantage to calculate the alloy system and transport properties [14,15]. However, these packages are more appropriate for numerical calculations rather than obtaining the Hamiltonians analytically. At present, a lot of researchers using symmetry adapted tight-binding model to investigate physical properties of electronic system [16–26]. However, most of the software packages are mainly focused on the tight-binding model for non-magnetic materials [27–31] and only a few of them can be used to construct the symmetry adapted tight-binding model automatically. For the first-principles level, Wannier90 can generate the Wannier-tight-binding model by interfacing with first-principles software, but the symmetry adapted Wannier function can not be applied to other first-principles software (such as VASP, ABINIT) except Quantum-Espresso [32–35]. FPLO can generate symmetry adapted tight-binding model with proper parameters for given structures [36]. Meanwhile, both Wannier90 and FPLO do not support magnetic symmetry. For the model level, GTPack, Qsymm and MathemaTB can generate the tight-binding model with space group symmetry but does not support magnetic symmetry directly [37–39]. WannierTools can do the symmetrization of non-magnetic tight-binding model but cannot generate the tight-binding model by itself [40].

Therefore, it is necessary to develop a package which can construct the tight-binding model with magnetic space group symmetry automatically. Here we introduce a software package: MagneticTB, a tool for generating the tight-binding model for the system with arbitrary magnetic space group. The required input information of this package is only the magnetic space group number and the orbital information in each Wyckoff positions. It can help to investigate the physical properties of the given symmetry. We also present some useful functions including get the matrix expression for symmetry operators, manipulate the band structure by parameters and interface with other software.

This paper is organized as follows. In Sec. 2, we give an introduction of symmetry adapted tight-binding methods. In Sec. 3, the usage of MagneticTB are given, including how to install and run MagneticTB. In Sec. 4, we give three concrete examples, such examples show the specific capabilities of the MagneticTB. Finally, conclusions are given.

2. Symmetry adapted tight-binding method

In periodic system, the bases of tight-binding model can be written as Bloch sum [16]

$$\psi^n_{lm\boldsymbol{k}}(\boldsymbol{r}) = \frac{1}{\sqrt{N}}\sum_{\boldsymbol{R}_j} e^{i\boldsymbol{k}\cdot(\boldsymbol{R}_j+\boldsymbol{d}^n_l)}\varphi^n_m(\boldsymbol{r}-\boldsymbol{R}_j-\boldsymbol{d}^n_l) \tag{1}$$

where N is the number of unit cells in the crystal, $\boldsymbol{R}_j$ is the translation vector of the Bravais lattice, $\boldsymbol{d}^n_l$ is the position of n-th Wyckoff position's l-th atom in the unit cell (for each Q and $\boldsymbol{d}^n_l$ there exists one and only one pair of $\boldsymbol{d}^n_{l'}$ and R' which satisfies $Q\boldsymbol{d}^n_l = \boldsymbol{d}^n_{l'} + R'$ where Q is arbitrary group element in the (magnetic) space group and R' is a lattice vector), $\varphi^n_m(\boldsymbol{r})$ is the m-th atomic orbital basis for position $\boldsymbol{d}^n_l$ but located at coordinate origin. Then Eq. (1) satisfies the Bloch theorem $\psi^n_{lm\boldsymbol{k}}(\boldsymbol{r}+\boldsymbol{R}_j) = e^{i\boldsymbol{k}\cdot\boldsymbol{R}_j}\psi^n_{lm\boldsymbol{k}}(\boldsymbol{r})$. The tight-binding Hamiltonian can be written as:

$$\begin{aligned} H^{nn'}_{lml'm'}(\boldsymbol{k}) &= \sum_{\boldsymbol{R}_j} e^{i\boldsymbol{k}\cdot(\boldsymbol{R}_j+\boldsymbol{d}^{n'}_{l'}-\boldsymbol{d}^n_l)} E_{mm'}(\boldsymbol{d}^n_l, \boldsymbol{R}_j+\boldsymbol{d}^{n'}_{l'}) \\ E_{mm'}(\boldsymbol{d}^n_l, \boldsymbol{R}_j+\boldsymbol{d}^{n'}_{l'}) &= \langle\varphi^n_m(\boldsymbol{r}-\boldsymbol{d}^n_l)|\hat{H}|\varphi^{n'}_{m'}(\boldsymbol{r}-\boldsymbol{d}^{n'}_{l'}-\boldsymbol{R}_j)\rangle \end{aligned} \tag{2}$$

for simplicity, we rewrite the atomic orbitals in vector form: $\Phi^n(\boldsymbol{r}-\boldsymbol{R}_j-\boldsymbol{d}^n_l) = \{\varphi^n_m(\boldsymbol{r}-\boldsymbol{R}_j-\boldsymbol{d}^n_l)\}, (m=1,...,M_n)$. Then $E_{mm'}(\boldsymbol{d}_j, \boldsymbol{R}_j+\boldsymbol{d}_{l'})$ $(m=1,...,M_n;\ m'=1,\ldots,M_{n'})$ form an $M_n \times M_{n'}$ matrix:

$$E(\boldsymbol{d}^n_l, \boldsymbol{R}_j+\boldsymbol{d}^{n'}_{l'}) = \langle\Phi^n(\boldsymbol{r}-\boldsymbol{d}^n_l)|\hat{H}|\Phi^{n'}(\boldsymbol{r}-\boldsymbol{R}_j-\boldsymbol{d}^{n'}_{l'})\rangle \tag{3}$$

Then the Hamiltonian can be rewritten as:

$$H^{nn'}_{ll'}(\boldsymbol{k}) = \sum_{\boldsymbol{R}_j} e^{i\boldsymbol{k}\cdot(\boldsymbol{R}_j+\boldsymbol{d}^{n'}_{l'}-\boldsymbol{d}^n_l)} E(\boldsymbol{d}^n_l, \boldsymbol{R}_j+\boldsymbol{d}^{n'}_{l'}) \tag{4}$$

$E(\boldsymbol{d}^n_l, \boldsymbol{R}_j+\boldsymbol{d}^{n'}_{l'})$ is the hopping matrix between n-th Wyckoff position's l-th atom to n'-th Wyckoff position's l'-th atom. When the lattice is in invariant under some symmetry $E(\boldsymbol{d}^n_l, \boldsymbol{R}_j+\boldsymbol{d}^{n'}_{l'})$ may be not independent for arbitrary $\boldsymbol{d}^n_l$ and $\boldsymbol{d}^{n'}_{l'}$. Fortunately, for symmetry operation Q, group representation theory gives us explicit expression for the relationship between $E(Q\boldsymbol{d}^n_j, Q(\boldsymbol{R}_j+\boldsymbol{d}^{n'}_{l'}))$ and $E(\boldsymbol{d}^n_j, \boldsymbol{R}_j+\boldsymbol{d}^{n'}_{l'})$.

For the case that symmetry operation does not contain the time reversal $\mathcal{T}$, i.e. $Q = \{R|\boldsymbol{t}\}$, where R and $\boldsymbol{t}$ are the rotation and translation part of Q respectively, we have

$$E(Q\boldsymbol{d}^n_l, Q(\boldsymbol{R}_j+\boldsymbol{d}^n_{l'})) = D^n(R)E(\boldsymbol{d}^n_l, \boldsymbol{R}_l+\boldsymbol{d}^{n'}_{l'})D^{n'\dagger}(R) \tag{5}$$

For the case that operation Q contains time reversal symmetry $\mathcal{T}$, i.e. $Q = \{R|\boldsymbol{t}\}\mathcal{T}$, we have

$$E(Q\boldsymbol{d}^n_l, Q(\boldsymbol{R}_j+\boldsymbol{d}^n_{l'})) = D^n(R\mathcal{T})E^*(\boldsymbol{d}^n_l, \boldsymbol{R}_j+\boldsymbol{d}^{n'}_{l'})D^{n'\dagger}(R\mathcal{T}) \tag{6}$$

Where $D^n(R)(D^n(R\mathcal{T}))$ are the $M_n \times M_n$ representation matrices of $R(R\mathcal{T})$ under atomic orbital bases $\Phi^n(\boldsymbol{r})$ (not necessarily irreducible representations), $E^*(\boldsymbol{d}^n_l, \boldsymbol{R}_j+\boldsymbol{d}^{n'}_{l'})$ is complex conjugate of $E(\boldsymbol{d}^n_l, \boldsymbol{R}_j+\boldsymbol{d}^{n'}_{l'})$ (see Fig. 1 for example). It is clear that for spinless cases with time-reversal symmetry $\mathcal{T}$, when the basis functions are real, $D(\mathcal{T})$ is equal to identity matrix, indicating that $E(\boldsymbol{d}^n_l, \boldsymbol{R}_j+\boldsymbol{d}^{n'}_{l'})$ are real matrices.

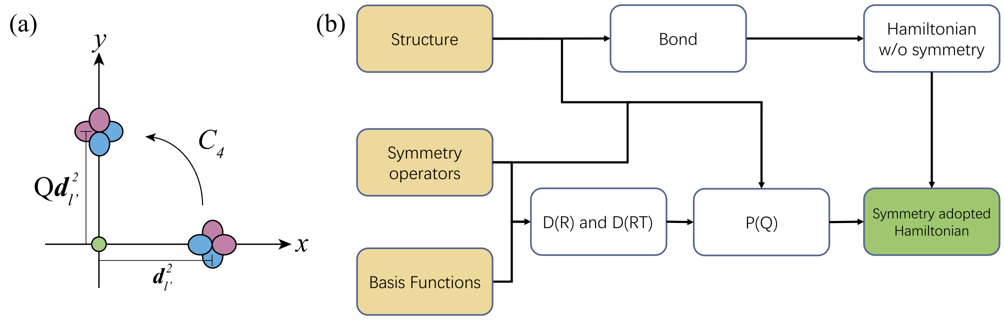

Fig. 1. (a) Sketch of relationship between $E(\boldsymbol{d}_j^n, \boldsymbol{R}_j + \boldsymbol{d}_{l'}^{n'})$ and $E(Q\boldsymbol{d}_j^n, Q(\boldsymbol{R}_j + \boldsymbol{d}_{l'}^{n'}))$, in this example we set $Q = C_4\mathcal{T}$, $\Phi^1(\mathbf{r}) = \{s\}$ locate at $\boldsymbol{d}_l^1 = (0,0)$, $\Phi^2(\mathbf{r}) = \{p_x, p_y\}$ locate at $\boldsymbol{d}_{l'}^2 = (\lambda, 0)(\lambda \neq 0)$. Then we have $D^1(C_4\mathcal{T}) = 1$, $D^2(C_4\mathcal{T}) = -i\sigma_y$, and $E(Q\boldsymbol{d}_l^1, Q\boldsymbol{d}_{l'}^2) = E^*(\boldsymbol{d}_l^1, \boldsymbol{d}_{l'}^2) \times (-i\sigma_y)$. (b) Workflow of MagneticTB.

The next step is to get the analytical expressions of $D^n(R)(D^n(R\mathcal{T}))$. For a fixed n, we don't have to worry about mixing superscripts of n in $D^n(R)$ because transformations can only occur under the same n. So we temporarily use $D(R)$ rather than $D^n(R)$ in this step. Consider the following four cases[1]

i. Spinless system and Q does not contain $\mathcal{T}$.
ii. Spinless system and Q contain $\mathcal{T}$.
iii. Spinful system and Q does not contain $\mathcal{T}$.
iv. Spinful system and Q contain $\mathcal{T}$.

In case i, $D(R)$ can be obtained simply by solve the linear equation [41]

$$\hat{R}\Phi(\mathbf{r}) = \Phi(R^{-1}\mathbf{r}) = \Phi(\mathbf{r})D(R) \tag{7}$$

in which $\hat{R}$ is the function operator for the rotation R. In case ii, we define $\overline{\Phi}(\mathbf{r}) = \hat{\mathcal{T}}\Phi(\mathbf{r})$, for spinless system $\mathcal{T} = \mathcal{K}$, with $\mathcal{K}$ indicating the complex conjugate operator. Hence, $\overline{\Phi}(\mathbf{r}) = \Phi^*(\mathbf{r})$ and then solve the linear equation

$$\hat{R}\hat{\mathcal{T}}\Phi(\mathbf{r}) = \overline{\Phi}(R^{-1}\mathbf{r}) = \Phi(\mathbf{r})D(R\mathcal{T}) \tag{8}$$

In case iii, since the spin matrix is orbital independent we define the basis function as

$$\Phi^s(\mathbf{r}) = \{\Phi(\mathbf{r})\uparrow, \Phi(\mathbf{r})\downarrow\} \tag{9}$$

The two spinors $\uparrow = (1,0)^T$ and $\downarrow = (0,1)^T$. Under the rotation $\hat{R}$ they are transformed according to

$$\hat{R}(\uparrow, \downarrow) = (\uparrow, \downarrow)D^{\frac{1}{2}}(R) \tag{10}$$

For proper rotation R, $D^{\frac{1}{2}}(R) = \exp(-\frac{1}{2}i\alpha\boldsymbol{n}\cdot\hat{\boldsymbol{\sigma}})$, where α is the rotation angle of R, $\boldsymbol{n}$ is the unit vector along rotation axis, for improper rotation S, $R = IS$, I is the inversion symmetry, $D^{\frac{1}{2}}(S) = D^{\frac{1}{2}}(R)$ [42]. Then $D(R)$ can be obtained by solving the linear equation

$$\hat{R}\Phi^s(\mathbf{r}) = \Phi^s(\mathbf{r})D(R) \tag{11}$$

Case (iv) is similar to case (ii), the only difference is replace the time-reversal operator $\mathcal{T} = \mathcal{K}$ by $\mathcal{T} = i\hat{\sigma}_y\mathcal{K}$ and consider the spin rotation matrices. The above four cases cover all the possibilities of $D(R)$ and $D(R\mathcal{T})$. It should be emphasized that case i and ii are valid for the system without considering spin, e.g. the phonon systems and the electronic systems with negligible spin-orbital coupling.

Then the operator (or representation matrix) for Q can be defined as

$$P_{ll'}^{nn'}(Q) = \begin{cases} \delta_{nn'}\tilde{\delta}_{\boldsymbol{d}_l^n, Q\boldsymbol{d}_{l'}^{n'}} D^n(R) & \text{Q does not contain } \mathcal{T} \\ \delta_{nn'}\tilde{\delta}_{\boldsymbol{d}_l^n, Q\boldsymbol{d}_{l'}^{n'}} D^n(R\mathcal{T}) & \text{Q contains } \mathcal{T} \end{cases} \tag{12}$$

where $\tilde{\delta}_{\boldsymbol{d}_l^n, Q\boldsymbol{d}_{l'}^{n'}}$ is equal to 1 only when d_l^n and $Qd_{l'}^{n'}$ differ by a lattice vector and to 0 otherwise (it can also be written as $\tilde{\delta}_{\boldsymbol{d}_l^n, Q\boldsymbol{d}_{l'}^{n'}} = \delta_{\boldsymbol{d}_l^n, Q\boldsymbol{d}_{l'}^{n'} + \boldsymbol{R}_s}$ if a suitable lattice vector $\boldsymbol{R}_s$ is chosen). The Hamiltonian under constraint of Q can be written as

$$P(Q)^{-1}H(\boldsymbol{k})P(Q) = H(R^{-1}\boldsymbol{k}) \tag{13}$$

for $Q = \{R|\boldsymbol{t}\}$, and

$$P(Q)^{-1}H(\boldsymbol{k})P(Q) = H^*(-R^{-1}\boldsymbol{k}) \tag{14}$$

[1] Here, spinless (spinful) means we consider the single (doubled)-valued representations of magnetic space group. That is, the rotation part of symmetry operations are members of (double) magnetic point group.

for $Q = \{R|\boldsymbol{t}\}\mathcal{T}$ [See Appendix A for proof of Eqs. (5)–(6) and Eqs. (13)–(14)]. Eqs. (13)–(14) are key point to generate the symmetry adapted tight-binding model. In MagneticTB we first generate the Hamiltonian with only translation symmetry and then use Eqs. (13)–(14) to the simplify the Hamiltonian (see Fig. 1(b)) for the workflow of MagneticTB]. The database for tight-binding model of 1651 magnetic space group can be found in our later work [43].

3. Capabilities of MagneticTB

3.1. Installation

To install the MagneticTB, unzip the "MagneticTB-main.zip" file and copy the MagneticTB directory to any of the following four paths:

- FileNameJoin[{**$UserBaseDirectory**, "Applications"}]
- FileNameJoin[{**$BaseDirectory**, "Applications"}]
- FileNameJoin[{**$InstallationDirectory**, "AddOns", "Packages"}]
- FileNameJoin[{**$InstallationDirectory**, "AddOns", "Applications"}]

Then one can use the package after running **Needs**["MagneticTB`"]. The version of Mathematica should higher or equal to 11.0.

3.2. Running

3.2.1. Core module

To initialize the program one should identify the magnetic space group and the orbital information in each Wyckoff positions. Here we provide a function msgop to show the symmetry information of an arbitrary magnetic space group. The only input of the msgop is the magnetic space group number, one can get the symmetry information by the following code:

```
msgop[gray[191]]
msgop[bnsdict[{191, 236}]]
msgop[ogdict[{191, 8, 1470}]]
Magnetic space group (BNS): {191.236,P6'/mm'm}
 Primitive  Lattice  vector:  {{a,0,0},{−a/2,(Sqrt[3]  a) /2,0},{0,0, c}}
Conventional Lattice  vector:  {{a,0,0},{−a/2,(Sqrt[3]  a) /2,0},{0,0, c}}
{{"1"   ,{{1,0,0},{0,1,0},{0,0,1}},{0,0,0},   F},
{"3z"  ,{{0,−1,0},{1,−1,0},{0,0,1}},{0,0,0},  F},
{"3z−1" ,{{−1,1,0},{−1,0,0},{0,0,1}},{0,0,0}, F},
{"2x" ,{{1,−1,0},{0,−1,0},{0,0,−1}},{0,0,0}, F},
 ...
```

here gray[191] return the magnetic space group code of gray space group 191, bnsdict[{191,236}] return the magnetic space group code of BNS No. 191.236, ogdict[{191,8,1470}] return the magnetic space group code of OG No. 191.8.1470. Then the msgop will print the standard lattice vector and the symmetry operations (for primitive cell) of the corresponding magnetic space group, which can be the input of the init function. Notice the magnetic space group code is build-in constant in MagneticTB, users should use gray, bnsdict, ogdict functions rather than inputting the magnetic space group code directly.

Then one can feed the above information to init function then the basic results of input structure can be generated. The init function have five mandatory options namely, lattice, lattpar, wyckoffposition, symminformation and basisFunctions (in ordinary Wolfram language the options for functions are optional, but such five options must be specified in MagneticTB in order to make the input clear). The lattice is the lattice vector of magnetic system which can contain parameters, lattpar is the parameters in lattice vector to determine the bond length of magnetic system, and wyckoffposition is a list to designate atomic position and magnetization-direction for each Wyckoff positions in the magnetic system. The format of wyckoffposition is:

$$\{\{\boldsymbol{a}_1, \boldsymbol{m}_1\}, \{\boldsymbol{a}_2, \boldsymbol{m}_2\}, \ldots\}$$

where $\boldsymbol{a}_i$ and $\boldsymbol{m}_i$ represent one of the atomic positions and its magnetization-directions of the i-th Wyckoff position, respectively. The symminformation contain the elements of the coset of magnetic space group with respect to translation group, which can direct use the output of msgop (notice that the output of msgop is standard symmetry operation from ISOTROPY [44,45]. However, users can also use the non-standard structure as input, not limit to the output of msgop). The format of symminformation is:

$$\{\{n_1, R_1, t_1, A_1\}, \{n_2, R_2, t_2, A_2\}, \ldots\}$$

where n_i is the name of symmetry operation, R_i and t_i are the rotation and translation part of symmetry operation, and A_i represents whether the symmetry operation is combined with time-reversal symmetry ("T" for true and "F" for false). Finally, the basisFunctions is the basis function for each Wyckoff position. The format of basisFunctions is:

$$\{b_1, b_2, \ldots\}$$

where b_i is the list of basis functions of the i-th Wyckoff position. The build-in basis functions for spinless case in MagneticTB is shown in Table 1.

When spin is considered, for build-in basis functions, add "up" or "dn" after basis functions string, e.g. for $|p_x \uparrow\rangle$, the basis function for spin-up case is "pxup". However, users may use other basis functions such as f, $|3/2, 1/2\rangle$ orbitals. In such cases, users can directly input the analytical expression of basis functions. For example, if only consider f_{xyz} orbital, one should input basisFunctions −> {{x∗y∗z}}. The analytical expressions of basis functions can be simply obtained from quantum mechanics or group theory books [37,46,47].

Table 1
String codes representing basis functions and available values for basisFunctions

Basis function	String	Basis function	String
s	"s"	p_x	"px"
p_y	"py"	p_z	"pz"
p_x+ip_y	"px+ipy"	p_x-ip_y	"px−ipy"
d_{z^2}	"dz2"	d_{xy}	"dxy"
d_{yz}	"dyz"	d_{xz}	"dxz"
$d_{x^2-y^2}$	"dx2−y2"		

Table 2
Basic results of init

properties	illustrate of properties
atompos	atomic position and magnetization-direction for each atom
wcc	$\boldsymbol{d}_l$ for each basis function
reclatt	reciprocal lattice vector for given structure
symmetryops	P_Q for each symmetry operation
unsymham[n]	generate the Hamiltonian for $(n-1)$-th neighbour hopping with only translation symmetry
symmcompile	summary of $P(Q)$, see main text for detail
bondclassify	summary of bonds information, see main text for detail
showbonds[n]	show the classification of the bonds for $(n-1)$-th neighbour

```
sgop=msgop[gray[191]];
 init [
 lattice  −> {{a,0,0},{−(a/2),(Sqrt[3] a) /2,0},{0,0, c }},
 lattpar  −> {a −> 1, c −> 3},
wyckoffposition −> {{{1/3, 2/3, 0}, {0, 0, 0}}},
symminformation −> sgop,
basisFunctions −> {{"pz"}}];
```

After inputting the above five options appropriately, one can run init and obtain the basic results. Here we introduce two important basic results: symmcompile and bondclassify, the other properties are given in Table 2. The format of symmcompile is

$$\{\{N_1,\{n_1,R_1,t_1,A_1\},P_1,R_1^k\},\{N_2,\{n_2,R_2,t_2,A_2\},P_2,R_2^k\},...\}$$

where N_i, P_i, R_i^k are the label, the symmetry operator (Eq. (12)) and the rotation acting on $\boldsymbol{k}$ space of the i-th symmetry operation, respectively. For example

```
symmcompile
{{1,{ "1"   ,{{1,0,0},{0,1,0},{0,0,1}},{0,0,0},   F },{{1,0},{0,1}},
       {{1,0,0},{0,1,0},{0,0,1}}},
{2,{ "6z"  ,{{1,−1,0},{1,0,0},{0,0,1}},{0,0,0},   F },{{0,1},{1,0}},
    {{0,−1,0},{1,1,0},{0,0,1}}},
 ...}
```

bondclassify provides the information of bond lengths and the classification of the bonds for the input structure. bondclassify[[i , j]] shows the bond information for the j-th atom's $(i-1)$-th neighbour ($i=1$ for on-site hopping). The format of bondclassify[[i , j]] is

$$\{l_i,n_{i,j},\{\{p_j,p_1'\},...,\{p_j,p_{n_{i,j}}'\}\}\}$$

where l_i is the bond length of the $(i-1)$-th neighbour hopping, $n_{i,j}$ is the number of bonds with bond length l_i and connecting to the j-th atom (note that l_i is defined globally for all atoms and hence $n_{i,j}=0$ may occur in certain cases). $\{p_j,p_k'\}$ gives the atomic positions of the two ends of the k-th bond ($k=1,\cdots,n_{i,j}$). One can use showbonds function to show the results of bondclassify. bondclassify is useful to analyse the bonds for the input structure.

Till this moment, symmetry adapted tight-binding model for magnetic system is ready to be generated. By using the symham[n] function, one can obtain the symmetry adapted tight-binding model. When $n=1$, symham[1] return the Hamiltonian with only on-site hopping, $n=2$ return the Hamiltonian with only nearest-neighbour hopping and so on. By default, MagneticTB will check all the input symmetry operations to ensure the Hamiltonian is correct. However, it may last long time when the structure is complex. In principle, only the generators of the (magnetic) space group are enough to get the Hamiltonian. Therefore, one can specify the symmetry operations by symmetryset−>list in symham where list is the list of indexes of the symmetry operations. For example, symham[2,symmetryset−>{2}] will generate the Hamiltonian with only C_{6z} symmetry for nearest-neighbour hopping. symmetryset can not only save computing resource but can also investigate the Hamiltonian for symmetry breaking cases. The parameters for each neighbour in MagneticTB are given in Table 3.

3.2.2. Plot module

After tight-binding model being generated, there may exist many parameters, one can use bandManipulate function to manipulate the band structure to investigate the relationship between band structure and parameters. The format of bandManipulate is

```
bandManipulate[{{{k1,k2},{name of k1, name of k2 }},...}, np,Hamiltonian]
```

Table 3
String codes representing n-th neighbour hoppings for symham

On-site energy	Nearest	Second-nearest	Third-nearest	$(k-1)$-th nearest
e1,e2,..	t1,t2 ,...	r1,r2 ,...	s1,s2 ,...	pkn1,pkn2,...

where np is the number of k points per line. Then one can easily check the band structure of different parameters. When the proper parameters are obtained, one can use bandplot to plot the band structure

```
bandplot[{{{k1,k2},{name of k1, name of k2 }},...}, np,Hamiltonian,parameters]
```

see section. 4 for concrete example.

3.2.3. IO module

In MagnetTB, one can get the tight-binding model for magnetic system. However, MagneticTB do not calculate the other properties (such as surface states, finding the band crossing points and so on) directly, since it will generally cost too much computing resources. It is better to do such heavy calculations by Fortran, Python or C. Therefore we develop hop function to convert the symmetry adapted tight-binding model to “wannier90_hr.dat” format, which is convenient to interface with WannierTools [40], Z2Pack [48], PythTB [49] and our home-made package Wannflow [50,51]. The “wannier90_hr.dat” in Wannier90 use the following convention [32], namely conventions II:

$$\begin{aligned}\tilde{\psi}^{n}_{lm\boldsymbol{k}}(\boldsymbol{r}) &= \frac{1}{\sqrt{N}}\sum_{\boldsymbol{R}_j} e^{i\boldsymbol{k}\cdot\boldsymbol{R}_j}\varphi^{n}_{lm}(\boldsymbol{r}-\boldsymbol{R}_j-\boldsymbol{d}^{n}_{l})\\ \tilde{H}^{nn'}_{lml'm'}(\boldsymbol{k}) &= \sum_{\boldsymbol{R}_j} e^{i\boldsymbol{k}\cdot\boldsymbol{R}_j}E_{mm'}(\boldsymbol{d}^{n}_{l},\boldsymbol{R}_j+\boldsymbol{d}^{n'}_{l'})\end{aligned} \tag{15}$$

which is different form MagneticTB in Eq. (2), the relationship between two conventions is

$$\begin{aligned}\tilde{H}(\boldsymbol{k}) &= V(\boldsymbol{k})H(\boldsymbol{k})V^{\dagger}(\boldsymbol{k})\\ V^{nn'}_{ll'}(\boldsymbol{k}) &= e^{i\boldsymbol{k}\cdot\boldsymbol{d}^{n}_{l}}\delta_{ll'}\delta_{nn'}\end{aligned} \tag{16}$$

In MagneticTB (convention I) the operation matrix defined in Eq. (12) is $\boldsymbol{k}$ independent while the Hamiltonian is non-periodic by shifting the reciprocal vector $\boldsymbol{G}$

$$H(\boldsymbol{k}+\boldsymbol{G}) = V^{\dagger}(\boldsymbol{G})H(\boldsymbol{k})V(\boldsymbol{G}) \tag{17}$$

By contrast, in conventions II the Hamiltonian is periodic i.e. $\tilde{H}(\boldsymbol{k}+\boldsymbol{G}) = \tilde{H}(\boldsymbol{k})$. The format of hop function is

```
hop[Hamiltonian,parameters]
```

See section. 4 for concrete example. One can also use symmhamII[ham] to generate the Wolfram expression for Hamiltonian in convention II. Notice that hop function (but not symmhamII) is only applied to the output of symham function, and that expressions explicitly including **Sin** or **Cos** may not work well.[2] Be careful to use it.

4. Examples

4.1. Graphene

Graphene with linear dispersion around Fermi level is one of the most important materials in spintronics [52]. The magnetic space group of graphene is $P6/mmm1'$ (BNS No. 191.234). There are two C atoms at $2c$ Wyckoff position, and the bands near Fermi energy are mainly from p_z orbital. The above information is enough to establish the tight-binding model near Fermi energy of graphene. The model can be obtained as follow

```
1  Needs["MagneticTB`"]
2  sgop = msgop[gray[191]];
3   init [
4   lattice  −> {{a,0,0},{−(a/2) ,( Sqrt[3]  a) /2,0},{0,0, c }},
5   lattpar  −> {a −> 1, c −> 3},
6  wyckoffposition  −> {{{1/3,  2/3,  0},  {0,  0,  0}}},
7  symminformation −> sgop,
8  basisFunctions −> {{"pz"}}];
9  ham = Sum[symham[i], {i, 3}]; MatrixForm[ham]
```

where the line 1 imports the MagneticTB package, line 2 reads the space group operations for graphene (191 is the space group number of graphene, one can also use sgop = msgop[bnsdict[{191,234}]]), line 3-8 set the structure and orbital information, and line 9 generates the symmetry adapted Hamiltonian up to second nearest neighbour hopping. The output of above script is:

[2] This is because we use the **Cases** command to grab the exponent value of e. Please use hop[output of symham,parameters] rather than hop[**FullSimplify**[output of symham],parameters].

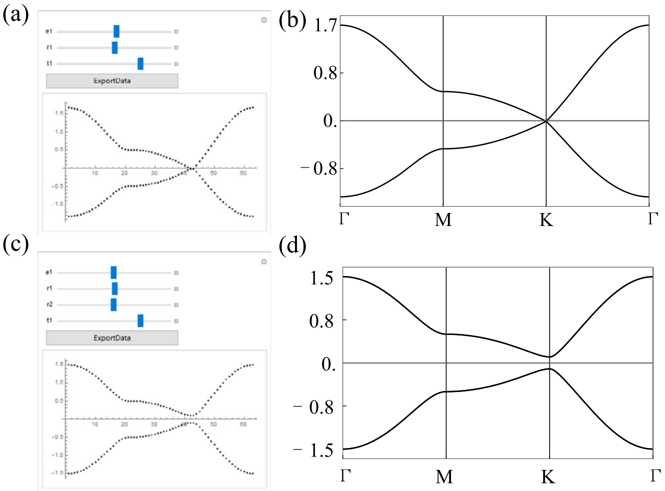

Fig. 2. Output of bandManipulate and bandplot for graphene without considering spin (a-b) and with spin (c-d).

$$\begin{bmatrix} e_1 + 2r_1(\cos(k_x+k_y)+\cos k_x+\cos k_y) & t_1 e^{i\left(-\frac{2k_x}{3}-\frac{k_y}{3}\right)} + t_1 e^{i\left(\frac{k_x}{3}-\frac{k_y}{3}\right)} + t_1 e^{i\left(\frac{k_x}{3}+\frac{2k_y}{3}\right)} \\ \dagger & e_1 + 2r_1(\cos(k_x+k_y)+\cos k_x+\cos k_y) \end{bmatrix}$$

For including spin-orbit coupling, the only thing which needs to change is the basis functions. That is, change the line 8 in the above script to

```
basisFunctions –> {{"pzup", "pzdn"}}];
```

and the corresponding Hamiltonian reads

$$\begin{bmatrix} e_1+h^- & 0 & h' & 0 \\ 0 & e_1+h^+ & 0 & h' \\ \dagger & 0 & e_1+h^+ & 0 \\ 0 & \dagger & 0 & e_1+h^- \end{bmatrix} \tag{18}$$

where $h^{\pm} = \pm 2r_1(\sin k_x + \sin k_y - \sin k_x + k_y) + 2r_2(\cos(k_x+k_y)+\cos k_x+\cos k_y)$, $h' = t_1 e^{i\left(-\frac{2k_x}{3}-\frac{k_y}{3}\right)} + t_1 e^{i\left(\frac{k_x}{3}-\frac{k_y}{3}\right)} + t_1 e^{i\left(\frac{k_x}{3}+\frac{2k_y}{3}\right)}$. Such model is corresponding to the first Z_2 topological insulator [6]. One can check the Hamiltonian by showing the bond lengths of $(i-1)$-th neighbour, e.g. the output of showbonds[3] is

2-th neighbour, Bond length = 1.		
Atom position	Num of bonds	pḱ
$\{\frac{1}{3}, \frac{2}{3}, 0\}$	6	$\{\{\frac{4}{3}, \frac{5}{3}, 0\}, \{\frac{4}{3}, \frac{2}{3}, 0\}, \{\frac{1}{3}, \frac{5}{3}, 0\}, \{\frac{1}{3}, -\frac{1}{3}, 0\}, \{-\frac{2}{3}, \frac{2}{3}, 0\}, \{-\frac{2}{3}, -\frac{1}{3}, 0\}\}$
$\{\frac{2}{3}, \frac{1}{3}, 0\}$	6	$\{\{\frac{5}{3}, \frac{4}{3}, 0\}, \{\frac{5}{3}, \frac{1}{3}, 0\}, \{\frac{2}{3}, \frac{4}{3}, 0\}, \{\frac{2}{3}, -\frac{2}{3}, 0\}, \{-\frac{1}{3}, \frac{1}{3}, 0\}, \{-\frac{1}{3}, -\frac{2}{3}, 0\}\}$

After getting the Hamiltonian, we can use bandManipulate and bandplot to plot the band structure, and click the "ExportData" button to print the value of parameters

```
1  path={
2      {{{0,0,0},{0,1/2,0}},{  "\[CapitalGamma]","M"}},
3      {{{0,1/2,0},{1/3,1/3,0}},{  "M","K"}},
4      {{{1/3,1/3,0},{0,0,0}},{  "K","\[CapitalGamma]"}}
5  };
6  bandManipulate[path, 20, ham]
7  bandManipulate[path, 20, hamsoc]
8  bandplot[path, 200, ham, {e1 –> 0, t1 –> 0.5, r1–> 0}]
9  bandplot[path, 200, hamsoc, {e1 –> 0, t1 –> 0.5, r1–> 0.02, r2–>0}]
```

where line 1-5 set the $\boldsymbol{k}$ path in the Brillouin zone, and line 6 and 8 (7 and 9) manipulate and show the band structure for the spinless (spinful) case (as shown in Fig. 2). Notice hamsoc is the output of symham with modified basis functions.

Moreover, we can get the "wannier90_hr.dat" by hop function for this model

```
hop[hamsoc, {e1 –> 0, r1 –> 0.02, r2 –> 0, t1 –> 0.5}]
Generated by MagneticTB
4
7
1    1    1    1    1    1    1
−1   −1    0    1    1    0.00000000    0.02000000
```

```
7   −1   −1    0    2    1    0.00000000   0.00000000
8   ...
```

where the list in line 1 means setting the parameters as $e_1 = 0, r_1 = 0.02, r_2 = 0, t_1 = 0.5$ in Eq. (18), line 2-8 is the tight-binding model in “wannier90_hr.dat” format.

4.2. Three-band tight-binding model for MoS$_2$

MoS$_2$ monolayer has direct bandgap in the visible range, strong spin-orbital coupling, and rich valley related physics, which make it an candidate for nanoelectronic, optoelectronic, and valleytronic applications [53,54]. The space group of MoS$_2$ is $P\bar{6}m2$ (space group No. 187). Considering the Mo atom at 1a Wyckoff position and using the d_{z^2}, d_{xy}, and $d_{x^2-y^2}$ orbitals, the model can be obtained by

```
1   sgop = msgop[gray[187]];
2   tran = {{1, −1, 0}, {0, 1, 0}, {0, 0, 1}};
3   sgoptr = MapAt[FullSimplify[tran.#.Inverse@tran] &, sgop, {;; , 2}];
4    init [
5      lattice  −> {{1, 0, 0}, {1/2, Sqrt[3]/2, 0}, {0, 0, 10}},
6      lattpar  −> {},
7     wyckoffposition −> {{{0, 0, 0}, {0, 0, 0}}},
8     symminformation −> sgoptr,
9     basisFunctions −> {{"dz2", "dxy", "dx2−y2"}}];
10  mos2 = Sum[symham[i, symmetryset −> {9, 11, 13}], {i, {1, 2}}];
11  mos2Liu = mos2 /. Thread[{kx, ky, kz} −> ({kx, ky, kz} (2 Pi)) .Inverse@reclatt];
```

where line 2-3 transfer the symmetry operations from the output of msgop to the convention described in Ref. [19], one can find how to do a general transformation in Ref. [55]. Line 10 shows the Hamiltonian in Cartesian coordinates. The output of above script gives exactly the same results as in Ref. [19]. The relationship of parameters between Ref. [19] and MagneticTB are

Ref. [19]	ϵ_1	ϵ_2	t_0	t_1	t_2	t_{11}	t_{12}	t_{22}
MagneticTB	e1	e2	t1	t2	t4	t3	t5	t6

4.3. Magnetic C-3 Weyl point

The charge-3 (C-3) Weyl point is a 0D two-fold band degeneracy with Chern number $|C| = 3$. Encyclopedia of emergent particles [56] tell us that the C-3 Weyl point always appear at least in a pair or coexist with nodal surface in nonmagnetic systems. Here we confirm that in magnetic system, due to the breaking of time reversal symmetry $\mathcal{T}$, the C-3 Weyl point can uniquely coexist with conventional Weyl points. Consider the type IV magnetic space group P_c3 (BNS No. 143.3). The generator of the group is C_{3z} and $\{E|00\frac{1}{2}\}\mathcal{T}$. Put $|p_x + ip_y \uparrow\rangle$, $|p_x - ip_y \downarrow\rangle$ basis functions at Wyckoff position 2a, and then the symmetry operator for C_{3z} and $E\{00\frac{1}{2}\}\mathcal{T}$ are

$$C_{3z} = -\sigma_z$$

$$\{E|00\frac{1}{2}\}\mathcal{T} = i\sigma_y$$

Under this bases the effective Hamiltonian at Γ point can be written as

$$H_{\text{C-3 WP}} = \epsilon + \alpha k_z \sigma_x + c k_\parallel^2 + \beta (k_x + e^{-i\frac{\pi}{3}} k_y)^3 \sigma_z + h.c. \tag{19}$$

where ϵ, c are real parameters and α, β are complex parameters. Besides, there are another three essential Weyl points locate at $(\pi, 0, 0)$, $(0, \pi, 0)$, $(\pi, \pi, 0)$. Since the C_{3z} symmetry does not change the Chern number of Weyl points, the Chern number at M has to be ± 1. According to Nielsen-Ninomiya no-go theorem [57,58], the Chern number of Γ is ∓ 3. One can easily check that the Chern number of Eq. (19) is ± 3. The degeneracies of Γ and M are because $(\{E|00\frac{1}{2}\}\mathcal{T})^2 = -1$ at $(0/\pi, 0/\pi, 0)$. The model can be obtained as follow

```
1   sgop = msgop[bnsdict[{143, 3}]];
2    init [ lattice  −> {{Sqrt[3]/2, −( 1/2), 0}, {0, 1, 0}, {0, 0, 2}},
3    lattpar  −> {},
4   wyckoffposition −> {{{0, 0, 0}, {0, 0, 1}}},
5   symminformation −> sgop,
6   basisFunctions −> {{{x + I y, 0}, {0, x − I y }}}];
7   c3w = Sum[symham[i], {i, {2, 4}}];
8   c3w2band = Table[c3w[[i, j ]], {i , {1, 4}}, {j , {1, 4}}];
```

Unlike the above two examples, we use the analytical expressions of basis functions $|x + iy \uparrow\rangle$ and $|x - iy \downarrow\rangle$ in line 6. Line 8 takes the elements in the four band Hamiltonian to obtain a two band Hamiltonian. This step is safe because $\{|x - iy \uparrow\rangle_1, |x + iy \downarrow\rangle_2\}$ (1 and 2 represent the first and second atom in the unit cell) can form a set of bases for the input structure. The band structure of c3w2band is shown in Fig. 3(a).

4.4. Magnetic cubic nodal-line

Topological high order nodal line is that the energy difference between the bands are non-linear, and the order of energy dispersion around the degeneracy points plays an important role in different physical properties, such as density of states, Berry phase and Landau-level [59]. Recently, Zhang et al. proposed high order nodal-line in magnetic system [60]. In this example, we use MagneticTB to generate

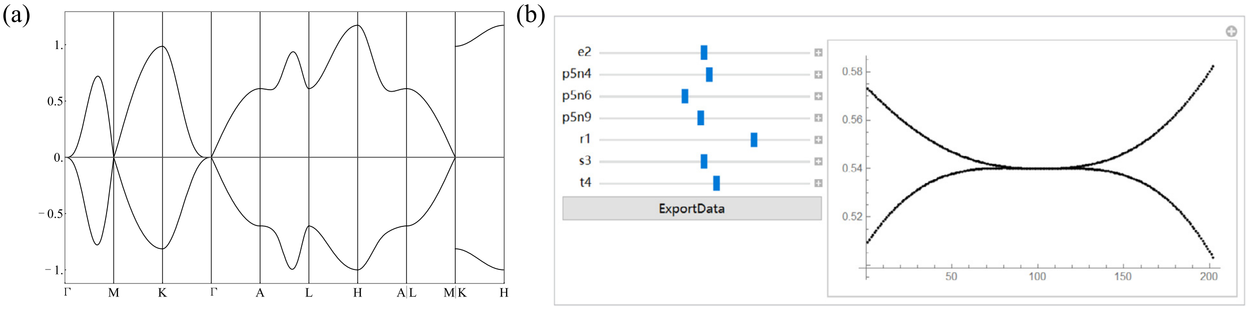

Fig. 3. (a) Output of bandplot for magnetic C-3 Weyl point, (b) Output of bandManipulate for magnetic cubic nodal-line.

magnetic cubic nodal-line. Generally, the magnetic cubic nodal-line is protected by C_{6z} and M_x symmetries, there are many magnetic space groups which contains the above two symmetries. Consider the type IV magnetic space group P_c6cc (BNS No. 184.196), and put $|p_x + ip_y \uparrow\rangle$, $|p_x - ip_y \downarrow\rangle$ basis functions at Wyckoff position $2a$. Then the tight-binding model can be generated by

```
sgop = msgop[bnsdict[{184, 196}]];
 init [ lattice  −> {{Sqrt[3]/2,  −1/2, 0},  {0,  1,  0},  {0,  0,  2}},
 lattpar  −> {},
wyckoffposition  −> {{{0,  0,  0},  {0,  0,  1}}},
symminformation −> sgop,
basisFunctions −> {{{x + I  y,  0},  {0,  x  − I y }}}];
cnl  = Sum[symham[i, symmetryset −> {2, 7, 13}], {i, 1, 5}];
cnl2band = Table[cnl[[ i ,  j ]],  { i ,  {1,  4}},  { j ,  {1,  4}}];
MatrixForm[cnl2band]
path = {{
{{0,  1/10,  1/4},  {0,  0,  1/4}},  {"Q",  "P"}},
 {{{0,  0,  1/4},  {−1/10, 1/10,  1/4}},  {"P",  "Q"}}};
bandManipulate[path, 20, cnl2band]
```

One can check that no mater how the parameters change, the dispersion of arbitrary point along Γ-A on k_x-k_y plane are non-linear, see Fig. 3(b) which is consistent with Ref. [60].

5. Conclusion

In conclusion, we have developed a software package to generate the symmetry-adapted tight-binding model for arbitrary magnetic space group. The input parameters for MagneticTB are clear and easy to set and both spinless and spinful Hamiltonian can be generated automatically. Besides, some useful functions such as manipulating the band structure, interfacing with other software are implemented, which can be used for further study on the magnetic systems. Moreover, MagneticTB can not only be used to investigate physical properties of electronic systems but also be used to study photonics, ultracold, acoustic, and mechanical systems [61–63]. Finally, an exciting direction for the future is to apply the magnetic field for the tight-binding model in MagneticTB [64].

Declaration of competing interest

The authors declare that they have no known competing financial interests or personal relationships that could have appeared to influence the work reported in this paper.

Acknowledgements

ZZ acknowledges the support by the NSF of China (Grant No. 12004028), the China Postdoctoral Science Foundation (Grant No. 2020M670106), the Fundamental Research Funds for the Central Universities (ZY2018). GBL acknowledges the support by the National Key R&D Program of China (Grant No. 2017YFB0701600). YY acknowledges the support by the National Key R&D Program of China (Grant No. 2020YFA0308800), the NSF of China (Grants Nos. 11734003, 12061131002), the Strategic Priority Research Program of Chinese Academy of Sciences (Grant No. XDB30000000).

Appendix A. Proof of Eqs. (5)–(6) and Eqs. (13)–(14)

In this appendix, we use the translation operation $T(\boldsymbol{d})$. For $Q = \{R|\boldsymbol{v}\}$, we have $QT(\boldsymbol{d}) = \{R|\boldsymbol{v}\}\{E|\boldsymbol{d}\} = \{R|R\boldsymbol{d} + \boldsymbol{v}\} = T(Q\boldsymbol{d})R$. Thus

$$\begin{aligned} E(\boldsymbol{d}_j^n, (\boldsymbol{R}_j + \boldsymbol{d}_{l'}^{n'})) &= \langle \hat{T}(\boldsymbol{d}_l^n)\Phi^n(\boldsymbol{r})|\hat{Q}^\dagger \hat{H}\hat{Q}|\hat{T}(\boldsymbol{d}_{l'}^{n'} + \boldsymbol{R}_j)\Phi^{n'}(\boldsymbol{r})\rangle \\ &= \langle \hat{Q}\hat{T}(\boldsymbol{d}_l^n)\Phi^n(\boldsymbol{r})|\hat{H}|\hat{Q}\hat{T}(\boldsymbol{d}_{l'}^{n'} + \boldsymbol{R}_j)\Phi^{n'}(\boldsymbol{r})\rangle \\ &= \langle \hat{T}(Q\boldsymbol{d}_l^n)R\Phi^n(\boldsymbol{r})|\hat{H}|\hat{T}(Q(\boldsymbol{d}_{l'}^{n'} + \boldsymbol{R}_j))R\Phi^{n'}(\boldsymbol{r})\rangle \\ &= D^{n\dagger}(R)\,\langle \hat{T}(Q\boldsymbol{d}_l^n)\Phi^n(\boldsymbol{r})|\hat{H}|\hat{T}(Q(\boldsymbol{d}_{l'}^{n'} + \boldsymbol{R}_j))\Phi^{n'}(\boldsymbol{r})\rangle\, D^{n'}(R) \\ &= D^{n\dagger}(R)E(Q\boldsymbol{d}_j^n, Q(\boldsymbol{R}_j + \boldsymbol{d}_{l'}^{n'}))D^{n'}(R) \end{aligned} \tag{A.1}$$

which completes the proof of Eq. (5).

For $Q = \{R|\boldsymbol{v}\}\mathcal{T}$, notice time-reversal symmetry does not change the real space coordinates, i.e. $\mathcal{T}\boldsymbol{d} = \boldsymbol{d}$, we have $Q\,T(\boldsymbol{d}) = \{R|\boldsymbol{v}\}\mathcal{T}\{E|\boldsymbol{d}\} = \{R|R\boldsymbol{d} + \boldsymbol{v}\}\mathcal{T} = T(Q\,\boldsymbol{d})R\mathcal{T}$. Use the fact that for anti-unitary operator $\hat{\mathcal{A}}$, $\langle \hat{\mathcal{A}}\psi|\hat{\mathcal{A}}\phi\rangle = \langle\psi|\phi\rangle^*$, then

$$\begin{aligned}
E^*(\boldsymbol{d}_j^n, (\boldsymbol{R}_j + \boldsymbol{d}_{l'}^{n'})) &= \langle \hat{Q}\,\hat{T}(\boldsymbol{d}_l^n)\Phi^n(\boldsymbol{r})|\hat{Q}\,\hat{H}|\hat{T}(\boldsymbol{d}_{l'}^{n'} + \boldsymbol{R}_j)\Phi^{n'}(\boldsymbol{r})\rangle \\
&= \langle \hat{Q}\,\hat{T}(\boldsymbol{d}_l^n)\Phi^n(\boldsymbol{r})|\hat{H}|\hat{Q}\,\hat{T}(\boldsymbol{d}_{l'}^{n'} + \boldsymbol{R}_j)\Phi^{n'}(\boldsymbol{r})\rangle \\
&= \langle \hat{T}(Q\,\boldsymbol{d}_l^n)R\mathcal{T}\Phi^n(\boldsymbol{r})|\hat{H}|\hat{T}(Q\,(\boldsymbol{d}_{l'}^{n'} + \boldsymbol{R}_j))R\mathcal{T}\Phi^{n'}(\boldsymbol{r})\rangle \\
&= D^{n\dagger}(R\mathcal{T})\,\langle \hat{T}(Q\,\boldsymbol{d}_l^n)\Phi^n(\boldsymbol{r})|\hat{H}|\hat{T}(Q\,(\boldsymbol{d}_{l'}^{n'} + \boldsymbol{R}_j))\Phi^{n'}(\boldsymbol{r})\rangle\, D^{n'}(R\mathcal{T}) \\
&= D^{n\dagger}(R\mathcal{T})E(Q\,\boldsymbol{d}_j^n, Q\,(\boldsymbol{R}_j + \boldsymbol{d}_{l'}^{n'}))D^{n'}(R\mathcal{T})
\end{aligned} \tag{A.2}$$

which completes the proof of Eq. (6).

Proof of Eq. (13),

$$\begin{aligned}
[H(\boldsymbol{k})P(Q)]_{ll'}^{nn'} &= \sum_{\mu\nu} H(\boldsymbol{k})_{l\mu}^{n\nu} P_{\mu l'}^{\nu n'}(Q) \\
&= \sum_{\mu\nu}\sum_{\boldsymbol{R}_j} e^{i\boldsymbol{k}\cdot(\boldsymbol{R}_j + \boldsymbol{d}_\mu^\nu - \boldsymbol{d}_l^n)} E(\boldsymbol{d}_l^n, \boldsymbol{R}_j + \boldsymbol{d}_\mu^\nu)\delta_{\nu n'}\delta_{\boldsymbol{d}_\mu^\nu, Q\,\boldsymbol{d}_{l'}^{n'} + \boldsymbol{R}_s} D^{n'}(R) \\
&= \sum_{\boldsymbol{R}_j} e^{i\boldsymbol{k}\cdot(\boldsymbol{R}_j + Q\,\boldsymbol{d}_{l'}^{n'} + \boldsymbol{R}_s - \boldsymbol{d}_l^n)} E(\boldsymbol{d}_l^n, \boldsymbol{R}_j + Q\,\boldsymbol{d}_{l'}^{n'} + \boldsymbol{R}_s)D^{n'}(R) \\
&\xlongequal{\boldsymbol{R}_j + \boldsymbol{R}_s \to R\boldsymbol{R}_j} \sum_{\boldsymbol{R}_j} e^{i\boldsymbol{k}\cdot R(\boldsymbol{R}_j + \boldsymbol{d}_{l'}^{n'} - Q^{-1}\boldsymbol{d}_l^n)} E(\boldsymbol{d}_l^n, Q\,(\boldsymbol{R}_j + \boldsymbol{d}_{l'}^{n'}))D^{n'}(R) \\
&\xlongequal{\text{use Eq. (5)}} \sum_{\boldsymbol{R}_j} e^{iR^{-1}\boldsymbol{k}\cdot(\boldsymbol{R}_j + \boldsymbol{d}_{l'}^{n'} - Q^{-1}\boldsymbol{d}_l^n)} D^n(R)E(Q^{-1}\boldsymbol{d}_l^n, \boldsymbol{R}_j + \boldsymbol{d}_{l'}^{n'})
\end{aligned} \tag{A.3}$$

$$\begin{aligned}
[P(Q)H(R^{-1}\boldsymbol{k})]_{ll'}^{nn'} &= \sum_{\mu\nu} P_{l\mu}^{n\nu}(Q)H(R^{-1}\boldsymbol{k})_{\mu l'}^{\nu n'} \\
&= \sum_{\mu\nu}\sum_{\boldsymbol{R}_j} \delta_{n\nu}\delta_{\boldsymbol{d}_l^n, Q\,\boldsymbol{d}_\mu^\nu + \boldsymbol{R}_s} D^n(R)e^{iR^{-1}\boldsymbol{k}\cdot(\boldsymbol{R}_j + \boldsymbol{d}_{l'}^{n'} - \boldsymbol{d}_\mu^\nu)} E(\boldsymbol{d}_\mu^\nu, \boldsymbol{R}_j + \boldsymbol{d}_{l'}^{n'}) \\
&= \sum_{\boldsymbol{R}_j} D^n(R)e^{iR^{-1}\boldsymbol{k}\cdot(\boldsymbol{R}_j + \boldsymbol{d}_{l'}^{n'} - Q^{-1}(\boldsymbol{d}_l^n - \boldsymbol{R}_s))} E(Q^{-1}(\boldsymbol{d}_l^n - \boldsymbol{R}_s), \boldsymbol{R}_j + \boldsymbol{d}_{l'}^{n'}) \\
&= \sum_{\boldsymbol{R}_j} e^{iR^{-1}\boldsymbol{k}\cdot(\boldsymbol{R}_j + \boldsymbol{d}_{l'}^{n'} - Q^{-1}\boldsymbol{d}_l^n + R^{-1}\boldsymbol{R}_s)} D^n(R)E(Q^{-1}\boldsymbol{d}_l^n - R^{-1}\boldsymbol{R}_s, \boldsymbol{R}_j + \boldsymbol{d}_{l'}^{n'}) \\
&= \sum_{\boldsymbol{R}_j} e^{iR^{-1}\boldsymbol{k}\cdot(\boldsymbol{R}_j + \boldsymbol{d}_{l'}^{n'} - Q^{-1}\boldsymbol{d}_l^n + R^{-1}\boldsymbol{R}_s)} D^n(R)E(Q^{-1}\boldsymbol{d}_l^n, \boldsymbol{R}_j + \boldsymbol{d}_{l'}^{n'} + R^{-1}\boldsymbol{R}_s) \\
&\xlongequal{\boldsymbol{R}_j + R^{-1}\boldsymbol{R}_s \to \boldsymbol{R}_j} \sum_{\boldsymbol{R}_j} e^{iR^{-1}\boldsymbol{k}\cdot(\boldsymbol{R}_j + \boldsymbol{d}_{l'}^{n'} - Q^{-1}\boldsymbol{d}_l^n)} D^n(R)E(Q^{-1}\boldsymbol{d}_l^n, \boldsymbol{R}_j + \boldsymbol{d}_{l'}^{n'})
\end{aligned} \tag{A.4}$$

In the above derivation we use the relation $Q^{-1}(\boldsymbol{d}_l^n - \boldsymbol{R}_s) = Q^{-1}\boldsymbol{d}_l^n - R^{-1}\boldsymbol{R}_s$ (Q^{-1} is not linear). Compare the last lines of the above two equations and we can find they are equal to each other, i.e.

$$[H(\boldsymbol{k})P(Q)]_{ll'}^{nn'} = [P(Q)H(R^{-1}\boldsymbol{k})]_{ll'}^{nn'} \quad \Rightarrow \quad H(\boldsymbol{k})P(Q) = P(Q)H(R^{-1}\boldsymbol{k}) \tag{A.5}$$

Proof of Eq. (14): similar to Eq. (A.3) and Eq. (A.4) we have

$$\begin{aligned}
[H(\boldsymbol{k})P(Q)]_{ll'}^{nn'} &= \sum_{\mu\nu} H(\boldsymbol{k})_{l\mu}^{n\nu} P_{\mu l'}^{\nu n'}(Q) \\
&= \sum_{\mu\nu}\sum_{\boldsymbol{R}_j} e^{i\boldsymbol{k}\cdot(\boldsymbol{R}_j + \boldsymbol{d}_\mu^\nu - \boldsymbol{d}_l^n)} E(\boldsymbol{d}_l^n, \boldsymbol{R}_j + \boldsymbol{d}_\mu^\nu)\delta_{\nu n'}\delta_{\boldsymbol{d}_\mu^\nu, Q\,\boldsymbol{d}_{l'}^{n'} + \boldsymbol{R}_s} D^{n'}(R\mathcal{T}) \\
&= \sum_{\boldsymbol{R}_j} e^{i\boldsymbol{k}\cdot(\boldsymbol{R}_j + Q\,\boldsymbol{d}_{l'}^{n'} + \boldsymbol{R}_s - \boldsymbol{d}_l^n)} E(\boldsymbol{d}_l^n, \boldsymbol{R}_j + Q\,\boldsymbol{d}_{l'}^{n'} + \boldsymbol{R}_s)D^{n'}(R\mathcal{T}) \\
&\xlongequal{\boldsymbol{R}_j + \boldsymbol{R}_s \to R\boldsymbol{R}_j} \sum_{\boldsymbol{R}_j} e^{i\boldsymbol{k}\cdot R(\boldsymbol{R}_j + \boldsymbol{d}_{l'}^{n'} - Q^{-1}\boldsymbol{d}_l^n)} E(\boldsymbol{d}_l^n, Q\,(\boldsymbol{R}_j + \boldsymbol{d}_{l'}^{n'}))D^{n'}(R\mathcal{T}) \\
&\xlongequal{\text{use Eq. (6)}} \sum_{\boldsymbol{R}_j} e^{iR^{-1}\boldsymbol{k}\cdot(\boldsymbol{R}_j + \boldsymbol{d}_{l'}^{n'} - Q^{-1}\boldsymbol{d}_l^n)} D^n(R\mathcal{T})E^*(Q^{-1}\boldsymbol{d}_l^n, \boldsymbol{R}_j + \boldsymbol{d}_{l'}^{n'})
\end{aligned} \tag{A.6}$$

$$\begin{aligned}
[P(Q)H^*(-R^{-1}\boldsymbol{k})]_{ll'}^{nn'} &= \sum_{\mu\nu} P_{l\mu}^{n\nu}(Q)H^*(-R^{-1}\boldsymbol{k})_{\mu l'}^{\nu n'} \\
&= \sum_{\mu\nu}\sum_{\boldsymbol{R}_j} \delta_{n\nu}\delta_{\boldsymbol{d}_l^n, Q\boldsymbol{d}_\mu^\nu+\boldsymbol{R}_s} D^n(R\mathcal{T})e^{iR^{-1}\boldsymbol{k}\cdot(\boldsymbol{R}_j+\boldsymbol{d}_{l'}^{n'}-\boldsymbol{d}_\mu^\nu)}E^*(\boldsymbol{d}_\mu^\nu, \boldsymbol{R}_j+\boldsymbol{d}_{l'}^{n'}) \\
&= \sum_{\boldsymbol{R}_j} D^n(R\mathcal{T})e^{iR^{-1}\boldsymbol{k}\cdot(\boldsymbol{R}_j+\boldsymbol{d}_{l'}^{n'}-Q^{-1}(\boldsymbol{d}_l^n-\boldsymbol{R}_s))}E^*(Q^{-1}(\boldsymbol{d}_l^n-\boldsymbol{R}_s), \boldsymbol{R}_j+\boldsymbol{d}_{l'}^{n'}) \\
&= \sum_{\boldsymbol{R}_j} e^{iR^{-1}\boldsymbol{k}\cdot(\boldsymbol{R}_j+\boldsymbol{d}_{l'}^{n'}-Q^{-1}\boldsymbol{d}_l^n+R^{-1}\boldsymbol{R}_s)}D^n(R\mathcal{T})E^*(Q^{-1}\boldsymbol{d}_l^n-R^{-1}\boldsymbol{R}_s, \boldsymbol{R}_j+\boldsymbol{d}_{l'}^{n'}) \\
&= \sum_{\boldsymbol{R}_j} e^{iR^{-1}\boldsymbol{k}\cdot(\boldsymbol{R}_j+\boldsymbol{d}_{l'}^{n'}-Q^{-1}\boldsymbol{d}_l^n+R^{-1}\boldsymbol{R}_s)}D^n(R\mathcal{T})E^*(Q^{-1}\boldsymbol{d}_l^n, \boldsymbol{R}_j+\boldsymbol{d}_{l'}^{n'}+R^{-1}\boldsymbol{R}_s) \\
&\overset{\boldsymbol{R}_j+R^{-1}\boldsymbol{R}_s\to\boldsymbol{R}_j}{=\!=\!=\!=\!=} \sum_{\boldsymbol{R}_j} e^{iR^{-1}\boldsymbol{k}\cdot(\boldsymbol{R}_j+\boldsymbol{d}_{l'}^{n'}-Q^{-1}\boldsymbol{d}_l^n)}D^n(R\mathcal{T})E^*(Q^{-1}\boldsymbol{d}_l^n, \boldsymbol{R}_j+\boldsymbol{d}_{l'}^{n'})
\end{aligned} \tag{A.7}$$

Compare the last lines of the above two equations and we can find they are equal to each other, i.e.

$$[H(\boldsymbol{k})P(Q)]_{ll'}^{nn'} = [P(Q)H^*(-R^{-1}\boldsymbol{k})]_{ll'}^{nn'} \quad \Rightarrow \quad H(\boldsymbol{k})P(Q) = P(Q)H^*(-R^{-1}\boldsymbol{k}) \tag{A.8}$$

It is easy to verify that for A, B not containing $\mathcal{T}$ and C, D containing $\mathcal{T}$, $P(Q)$ obey the following corepresentation algebra:

$$\begin{aligned}
P(A)P(B) &= P(AB) \\
P(A)P(C) &= P(AC) \\
P(C)P^*(A) &= P(CA) \\
P(C)P^*(D) &= P(CD)
\end{aligned} \tag{A.9}$$

References

[1] P.R. Wallace, Phys. Rev. 71 (1947) 622.
[2] P.-O. Löwdin, J. Chem. Phys. 18 (1950) 365.
[3] J.C. Slater, G.F. Koster, Phys. Rev. 94 (1954) 1498.
[4] C.M. Goringe, D.R. Bowler, E. Hernández, Rep. Prog. Phys. 60 (1997) 1447.
[5] B.J. Wieder, B. Bradlyn, Z. Wang, J. Cano, Y. Kim, H.-S.D. Kim, A.M. Rappe, C.L. Kane, B.A. Bernevig, Science 361 (2018) 246.
[6] C.L. Kane, E.J. Mele, Phys. Rev. Lett. 95 (2005) 146802.
[7] L. Fu, Phys. Rev. Lett. 106 (2011) 106802.
[8] A.A. Burkov, M.D. Hook, L. Balents, Phys. Rev. B 84 (2011) 235126.
[9] C. Fang, M.J. Gilbert, B.A. Bernevig, Phys. Rev. B 88 (2013) 085406.
[10] C.-X. Liu, Antiferromagnetic crystalline topological insulators, arXiv:1304.6455 [cond-mat], 2013.
[11] O.K. Andersen, O. Jepsen, Phys. Rev. Lett. 53 (1984) 2571–2574.
[12] G. Krier, O. Jepsen, A. Burkhardt, O. Andersen, The TB-LMTO-ASA program, Stuttgart, www2.fkf.mpg.de/andersen/LMTODOC/LMTODOC.html, April 1995.
[13] B. Hourahine, B. Aradi, V. Blum, F. Bonafé, A. Buccheri, C. Camacho, C. Cevallos, M.Y. Deshaye, T. Dumitrică, A. Dominguez, S. Ehlert, M. Elstner, T. van der Heide, J. Hermann, S. Irle, J.J. Kranz, C. Köhler, T. Kowalczyk, T. Kubař, I.S. Lee, V. Lutsker, R.J. Maurer, S.K. Min, I. Mitchell, C. Negre, T.A. Niehaus, A.M.N. Niklasson, A.J. Page, A. Pecchia, G. Penazzi, M.P. Persson, J. Řezáč, C.G. Sánchez, M. Sternberg, M. Stöhr, F. Stuckenberg, A. Tkatchenko, V.W.-z. Yu, T. Frauenheim, J. Chem. Phys. 152 (2020) 124101.
[14] R. Zeller, P.H. Dederichs, B. Újfalussy, L. Szunyogh, P. Weinberger, Phys. Rev. B 52 (1995) 8807.
[15] H. Ebert, et al., The Munich SPR-KKR package, www.ebert.cup.uni-muenchen.de, 2017.
[16] R.F. Egorov, B.I. Reser, V.P. Shirokovskii, Phys. Status Solidi B 26 (1968) 391.
[17] V.N. Kuznetsov, A.N. Men, Phys. Status Solidi B 85 (1978) 95.
[18] W. Ku, H. Rosner, W.E. Pickett, R.T. Scalettar, Phys. Rev. Lett. 89 (2002) 167204.
[19] G.-B. Liu, W.-Y. Shan, Y. Yao, W. Yao, D. Xiao, Phys. Rev. B 88 (2013) 085433.
[20] B.J. Wieder, C.L. Kane, Phys. Rev. B 94 (2016) 155108.
[21] Z. Wang, A. Alexandradinata, R.J. Cava, B.A. Bernevig, Nature 532 (2016) 189.
[22] Z. Song, Z. Fang, C. Fang, Phys. Rev. Lett. 119 (2017) 246402.
[23] Z. Zhang, Q. Gao, C.-C. Liu, H. Zhang, Y. Yao, Phys. Rev. B 98 (2018) 121103(R).
[24] D. Gresch, Q. Wu, G.W. Winkler, R. Häuselmann, M. Troyer, A.A. Soluyanov, Phys. Rev. Mater. 2 (2018) 103805.
[25] M. Koshino, N.F.Q. Yuan, T. Koretsune, M. Ochi, K. Kuroki, L. Fu, Phys. Rev. X 8 (2018) 031087.
[26] Z.-M. Yu, W. Wu, Y.X. Zhao, S.A. Yang, Phys. Rev. B 100 (2019) 041118(R).
[27] B. Di Martino, M. Celino, V. Rosato, Comput. Phys. Commun. 120 (1999) 255.
[28] C.W. Groth, New J. Phys. 16 (2014) 063065.
[29] A.R. Supka, T.E. Lyons, L. Liyanage, P. D'Amico, R. Al Rahal Al Orabi, S. Mahatara, P. Gopal, C. Toher, D. Ceresoli, A. Calzolari, S. Curtarolo, M.B. Nardelli, M. Fornari, Comput. Mater. Sci. 136 (2017) 76.
[30] M. Nakhaee, S.A. Ketabi, F.M. Peeters, Comput. Phys. Commun. 254 (2020) 107379.
[31] M. Klymenko, J. Vaitkus, J. Smith, J. Cole, Comput. Phys. Commun. 259 (2021) 107676.
[32] A.A. Mostofi, J.R. Yates, Y.-S. Lee, I. Souza, D. Vanderbilt, N. Marzari, Comput. Phys. Commun. 178 (2008) 685.
[33] P. Giannozzi, S. Baroni, N. Bonini, M. Calandra, R. Car, C. Cavazzoni, D. Ceresoli, G.L. Chiarotti, M. Cococcioni, I. Dabo, A.D. Corso, S.d. Gironcoli, S. Fabris, G. Fratesi, R. Gebauer, U. Gerstmann, C. Gougoussis, A. Kokalj, M. Lazzeri, L. Martin-Samos, N. Marzari, F. Mauri, R. Mazzarello, S. Paolini, A. Pasquarello, L. Paulatto, C. Sbraccia, S. Scandolo, G. Sclauzero, A.P. Seitsonen, A. Smogunov, P. Umari, R.M. Wentzcovitch, J. Phys. Condens. Matter 21 (2009) 395502.
[34] G. Kresse, J. Furthmüller, Phys. Rev. B 54 (1996) 11169.
[35] X. Gonze, B. Amadon, P.M. Anglade, J.M. Beuken, F. Bottin, P. Boulanger, F. Bruneval, D. Caliste, R. Caracas, M. Côté, T. Deutsch, L. Genovese, P. Ghosez, M. Giantomassi, S. Goedecker, D.R. Hamann, P. Hermet, F. Jollet, G. Jomard, S. Leroux, M. Mancini, S. Mazevet, M.J.T. Oliveira, G. Onida, Y. Pouillon, T. Rangel, G.M. Rignanese, D. Sangalli, R. Shaltaf, M. Torrent, M.J. Verstraete, G. Zerah, J.W. Zwanziger, Comput. Phys. Commun. 180 (2009) 2582.

[36] K. Koepernik, H. Eschrig, Phys. Rev. B 59 (1999) 1743.
[37] W. Hergert, R. Geilhufe, Group Theory in Solid State Physics and Photonics: Problem Solving with Mathematica, Wiley-VCH Verlag GmbH & Co. KGaA, Weinheim, Germany, 2018.
[38] D. Varjas, T.Ö. Rosdahl, A.R. Akhmerov, New J. Phys. 20 (2018) 093026.
[39] P.H. Jacobse, Comput. Phys. Commun. 244 (2019) 392.
[40] Q. Wu, S. Zhang, H.-F. Song, M. Troyer, A.A. Soluyanov, Comput. Phys. Commun. 224 (2018) 405.
[41] J.D. Cloizeaux, Phys. Rev. 129 (1963) 554.
[42] CHAPTER VIII - SPIN, Quantum Mechanics, third edition, L.D. Landau, E.M. Lifshitz (Eds.), Pergamon, 1977.
[43] Z. Zhang, et al., Database for tight-binding model with magnetic symmetry, 2021, in preparation.
[44] D.B. Litvin, 1-, 2- and 3-Dimensional Magnetic Subperiodic Groups and Magnetic Space Groups, 2014.
[45] H.T. Stokes, D.M. Hatch, B.J. Campbell, ISOTROPY Software Suite, 2021, iso.byu.edu.
[46] C. Bradley, A. Cracknell, The Mathematical Theory of Symmetry in Solids: Representation Theory for Point Groups and Space Groups, Oxford University Press, New York, 1972.
[47] M.S. Dresselhaus, G. Dresselhaus, A. Jorio, Group Theory: Application to the Physics of Condensed Matter, Springer-Verlag, Berlin, 2008.
[48] D. Gresch, G. Autès, O.V. Yazyev, M. Troyer, D. Vanderbilt, B.A. Bernevig, A.A. Soluyanov, Phys. Rev. B 95 (2017) 075146.
[49] T. Yusufaly, D. Vanderbilt, S. Coh, Tight-Binding Formalism in the Context of the PythTB Package, 2017.
[50] Z. Zhang, R.-W. Zhang, X. Li, K. Koepernik, Y. Yao, H. Zhang, J. Phys. Chem. Lett. 9 (2018) 6224.
[51] X. Li, Z. Zhang, Y. Yao, H. Zhang, 2D Mater. 5 (2018) 045023.
[52] A.H. Castro Neto, F. Guinea, N.M.R. Peres, K.S. Novoselov, A.K. Geim, Rev. Mod. Phys. 81 (2009) 109.
[53] Q.H. Wang, K. Kalantar-Zadeh, A. Kis, J.N. Coleman, M.S. Strano, Nat. Nanotechnol. 7 (2012) 699.
[54] G.-B. Liu, D. Xiao, Y. Yao, X. Xu, W. Yao, Chem. Soc. Rev. 44 (2015) 2643.
[55] G.-B. Liu, M. Chu, Z. Zhang, Z.-M. Yu, Y. Yao, Comput. Phys. Commun. 265 (2021) 107993.
[56] Z.-M. Yu, Z. Zhang, G.-B. Liu, W. Weikang, X.-P. Li, Z. Run-Wu, S.A. Yang, Y. Yao, Encyclopedia of emergent particles in three-dimensional crystals, arXiv:2102.01517, 2020.
[57] H.B. Nielsen, M. Ninomiya, Nucl. Phys. B 185 (1981) 20.
[58] H.B. Nielsen, M. Ninomiya, Nucl. Phys. B 193 (1981) 173.
[59] Z.-M. Yu, W. Wu, X.-L. Sheng, Y.X. Zhao, S.A. Yang, Phys. Rev. B 99 (2019) 121106(R).
[60] Z. Zhang, Z.-M. Yu, S.A. Yang, Phys. Rev. B 103 (2021) 115112.
[61] T. Ozawa, H.M. Price, A. Amo, N. Goldman, M. Hafezi, L. Lu, M.C. Rechtsman, D. Schuster, J. Simon, O. Zilberberg, I. Carusotto, Rev. Mod. Phys. 91 (2019) 015006.
[62] N.R. Cooper, J. Dalibard, I.B. Spielman, Rev. Mod. Phys. 91 (2019) 015005.
[63] G. Ma, M. Xiao, C.T. Chan, Nat. Rev. Phys. 1 (2019) 281.
[64] R. Peierls, Z. Phys. 80 (1933) 763–791.